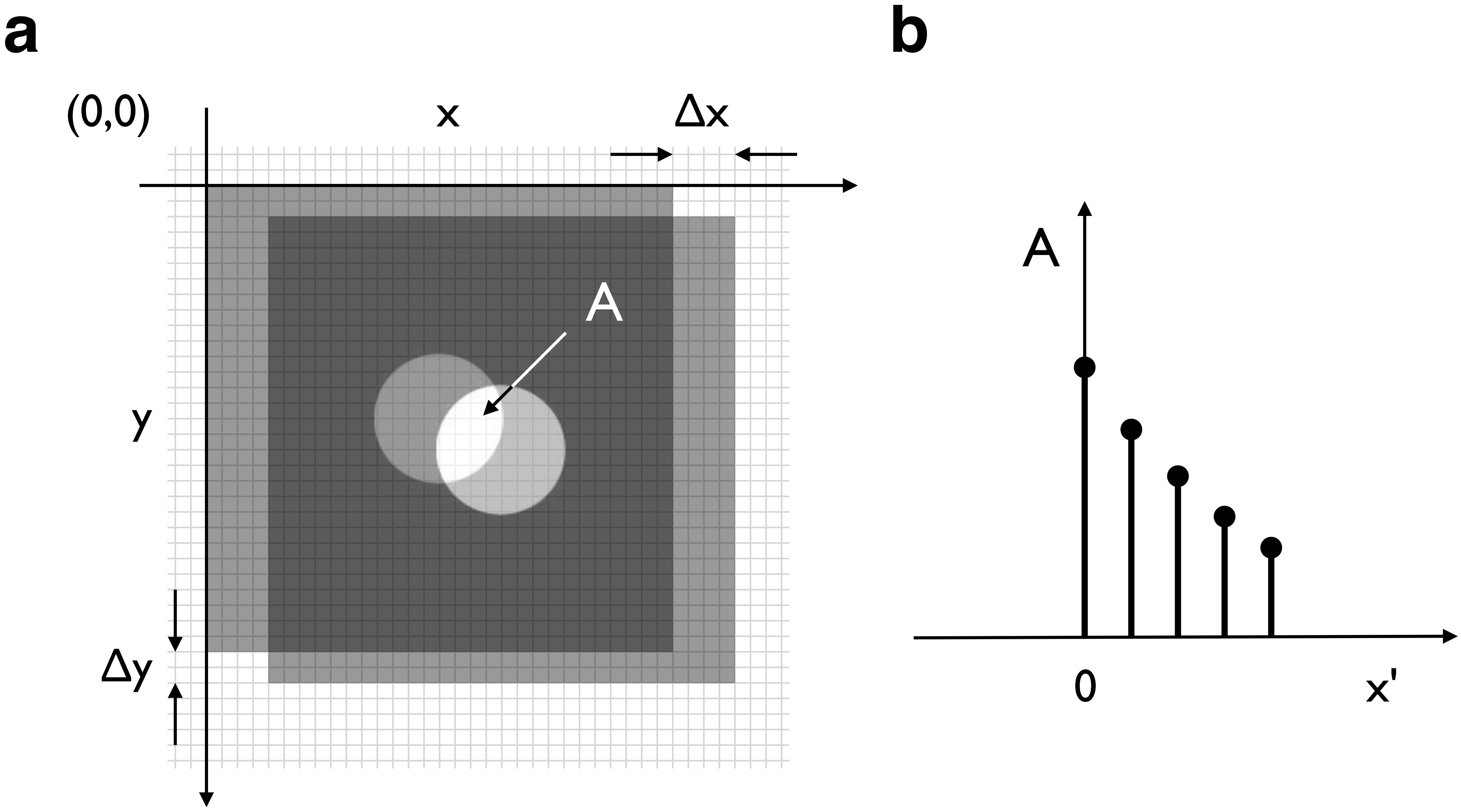

Figure 20.1
Visualization of the autocorrelation function.
(a) Two copies of an image are superposed, one copy is shifted in x- and y-direction by Δx and Δy; A = area of overlap of circles;
(b) the correlation between the image and its copy is measured as A(x'), the area of overlap as a function of x-displacement.

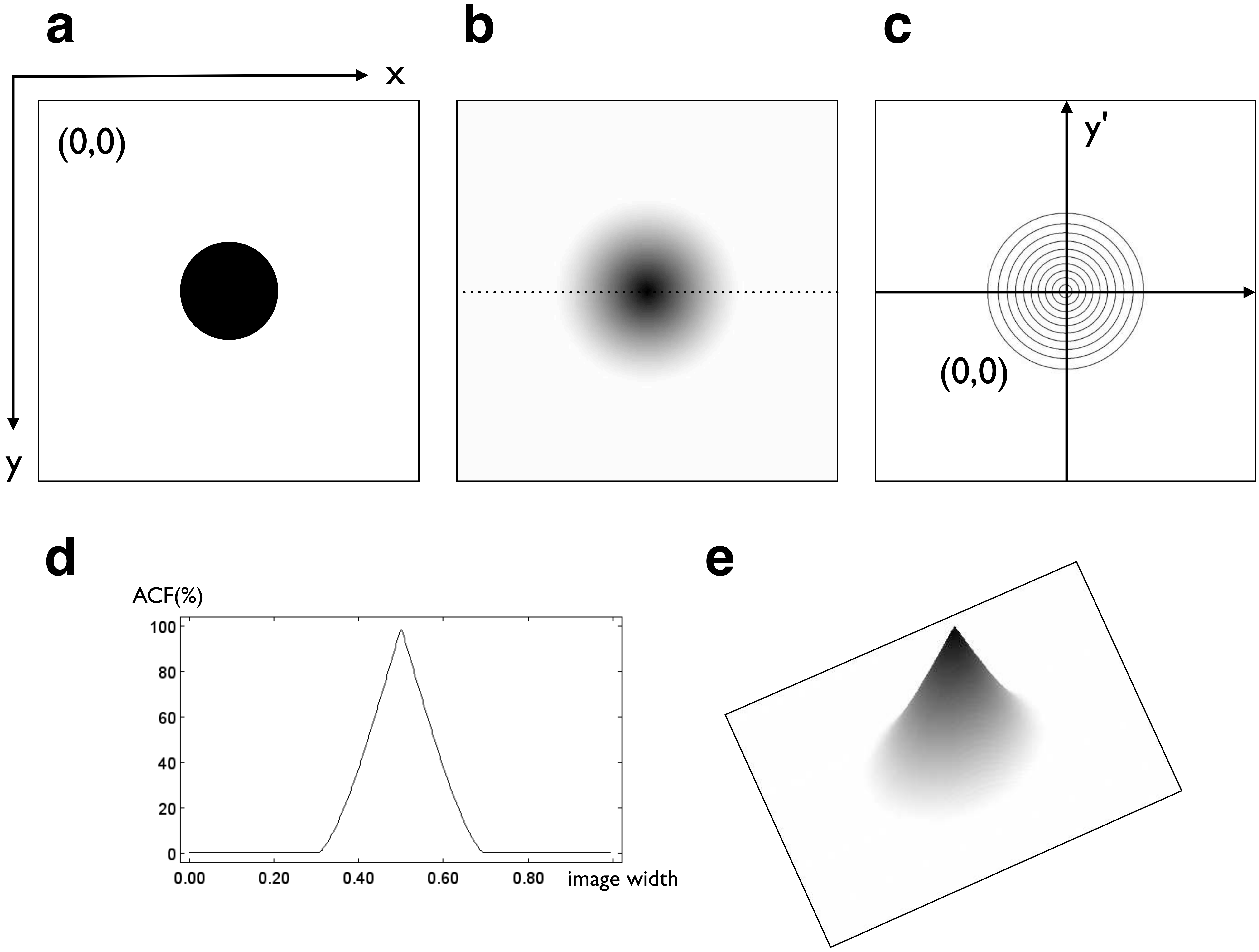

Figure 20.2
The autocorrelation function.
(a) Original image; x, y = dimensions of image plane; origin in upper left;
(b) image of autocorrelation function (ACF) of (a); stippled = trace of profile shown in (d);
(c) contour plot of ACF; contour level at 10%, 20%, etc. of maximum of ACF; origin of coordinate system in the center;
x', y' = displacement in x-, y- direction , same scaling as x-, y- coordinates of image;
(d) profile across ACF along trace shown in (b);
(e) topographic representation of ACF.

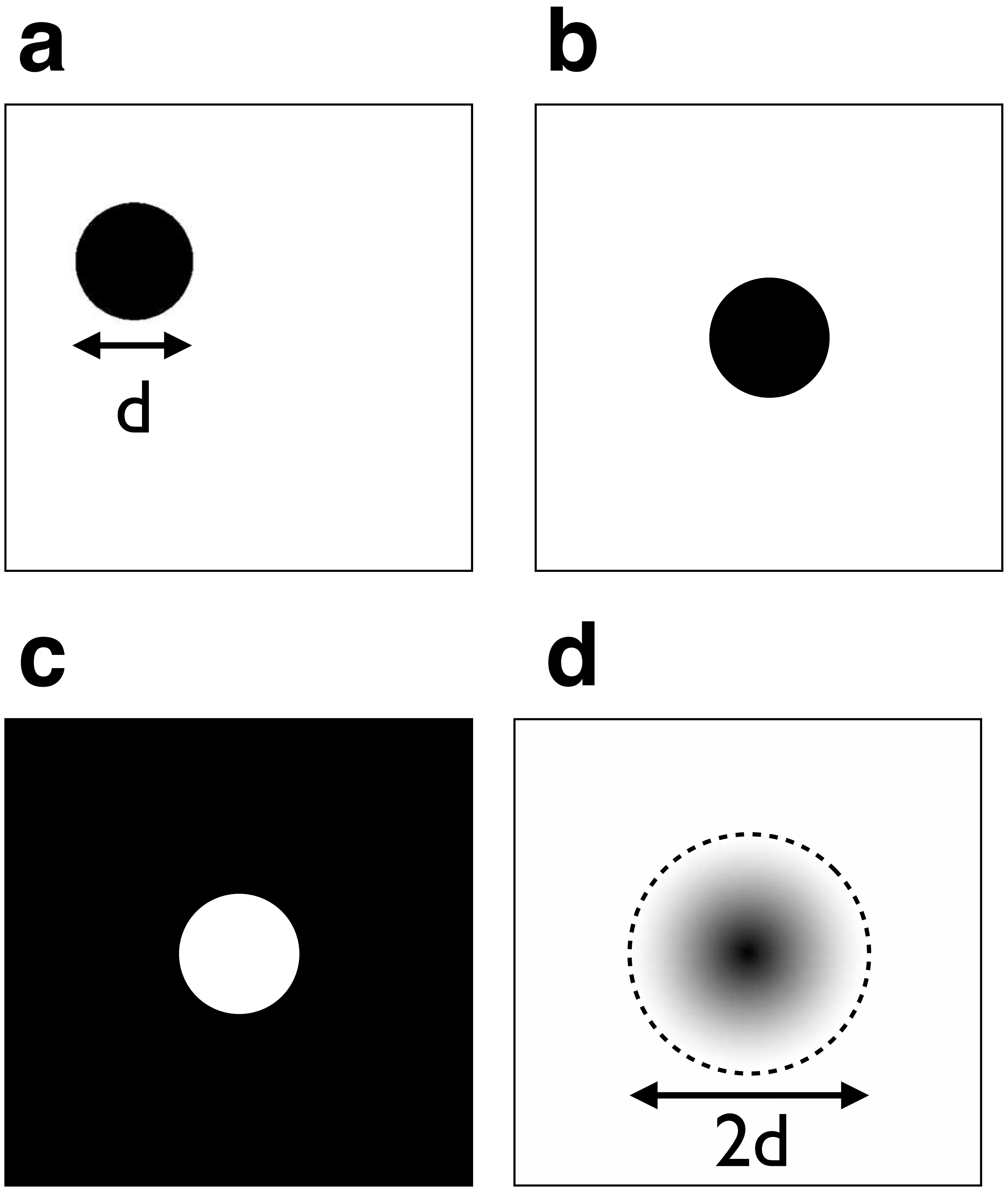

Figure 20.3
Geometric properties of autocorrelation function.
(a) Image of circle, diameter, d, indicated by double arrow;
(b) same circle as (a) moved to center;
(c) same as (b) with inverted contrast;
(d) autocorrelation function (ACF) is the same for (a), (b) and (c); base line (where ACF = 0) is indicated by stipples.
Note that the diameter of the base line is twice the diameter of the circle.

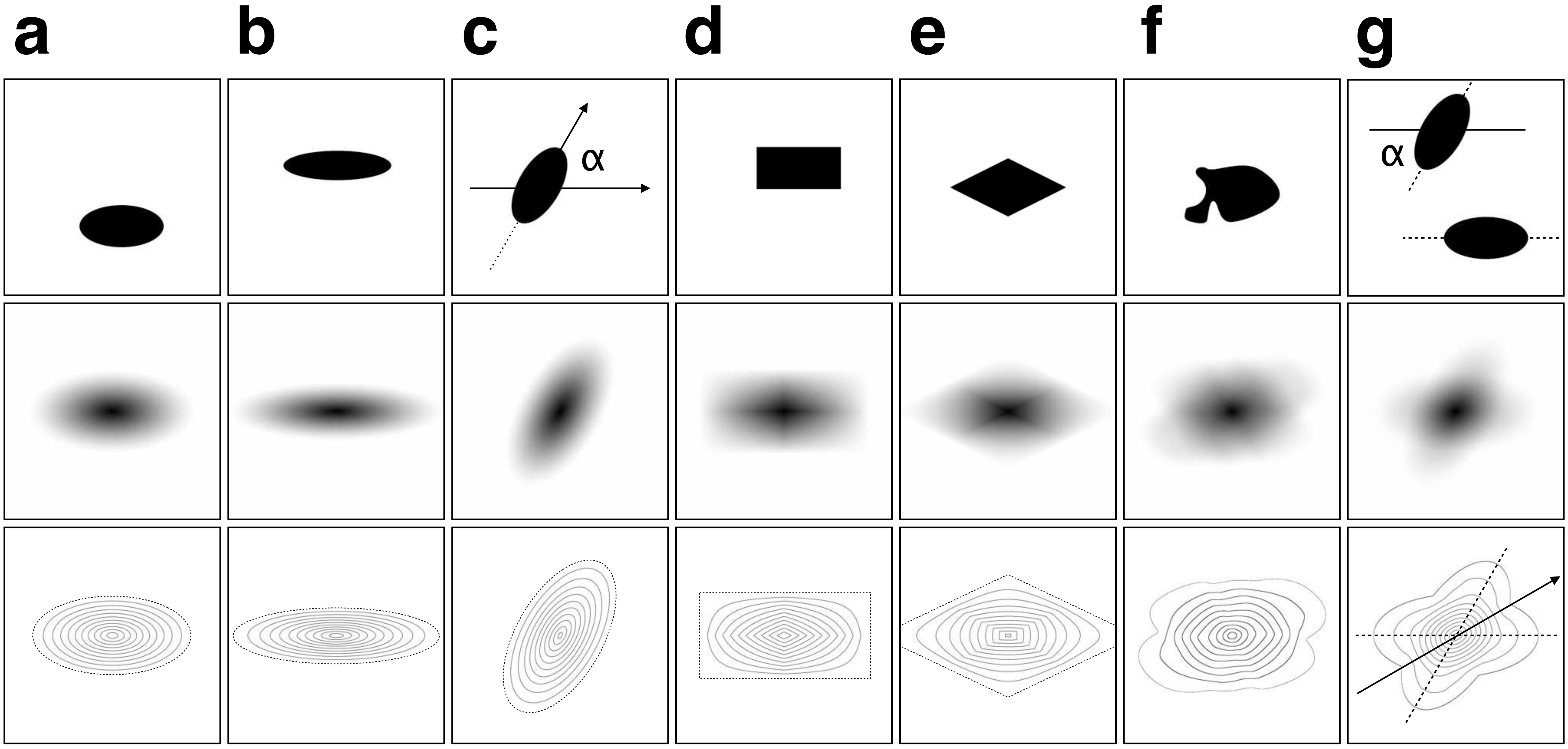

Figure 20.4
Autocorrelation function of individual shapes.
In each case, the image is shown (top) with the ACF (middle) and contour plots of the ACF (bottom); contours every 10% of ACF.
(a) Ellipse: b/a = 0.50, α = 0°;
(b) ellipse: b/a = 0.25, α = 0°;
(c) ellipse: b/a = 0.50, α = 60°;
(d) rectangle, b/a = 0.50, α = 0°;
(e) rhomb, b/a = 0.50, α = 0°;
(f) general shape;
(g) two ellipses, b/a = 0.50, α = 0° and α = 60°;
a = long axis; b = short axis; α = orientation of long axis, anticlockwise from positive x-axis.

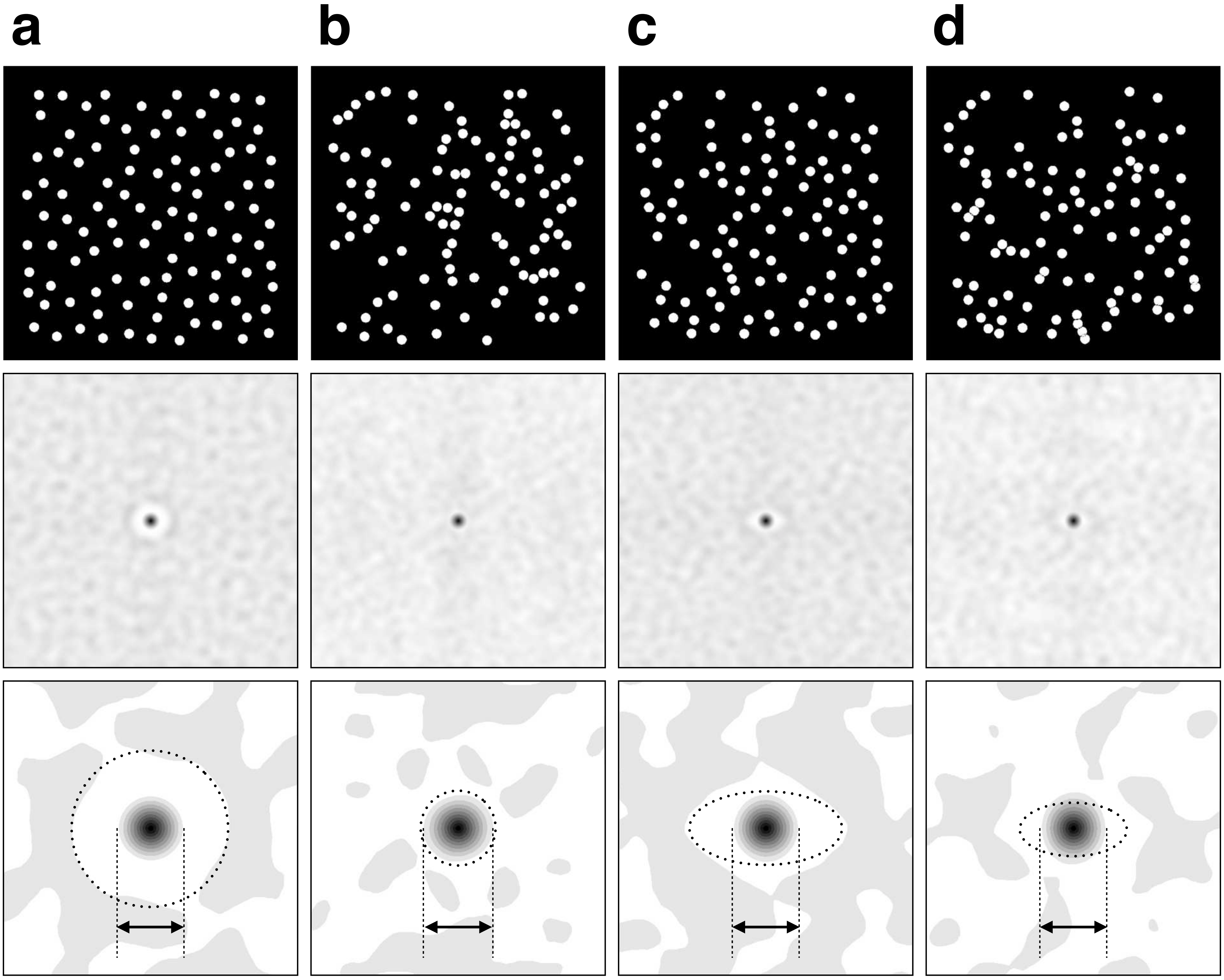

Figure 20.5
Influence of spacing on autocorrelation function.
100 circles (diameter, d) are randomly distributed in the image plane (top); the minimal distance between center points is d_{min}. The ACF is shown at the same scale (middle) and 4 times enlarged (bottom) with the anti-correlating distance shown as stippled outline.
(a) Isotropic distribution of center points with d_{min} = d;
(b) same as (a) with d_{min} = d/2; circles may touch;
(c) anisotropic distribution of center points: in x-direction: d_{min} = d; in y-direction: d_{min} = d/2; ratio = 2:1;
(d) same as (c): in x-direction: d_{min} = 2d/3; in y-direction: d_{min} = d/3; ratio = 2:1.

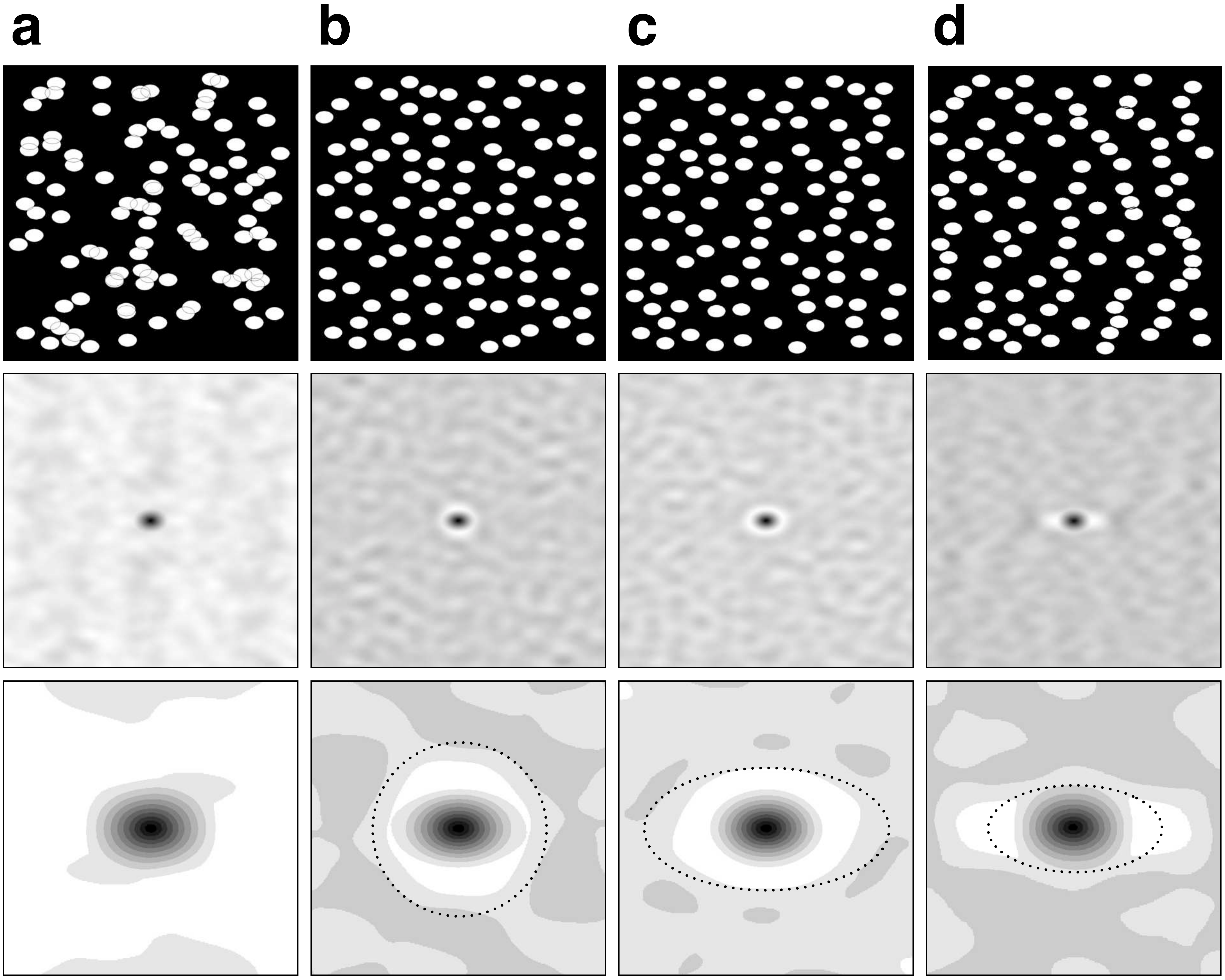

Figure 20.6
Influence of spacing on autocorrelation of ellipses.
100 identical ellipses are distributed in the image plane (top), for all, $b/a = 0.70$, $\alpha = 0°$. The ACF is shown at the same scale (middle) and 4 times enlarged (bottom) with the anti-correlating distance shown as stippled outline.
(a) Perfectly random distribution (Poisson distribution) of center points, note overlaps;
(b) random anti-correlated distribution of center points with $d_{min} = a$; ellipses may touch but not overlap;
(c) random anti-correlated distribution of center points, distribution is anisotropic: in x-direction: $d_{min} = \sqrt{2}a$; in y-direction: $d_{min} = a/\sqrt{2}$; ratio = 2:1;
(d) random anti-correlated distribution of center points, distribution is anisotropic: in x-direction: $d_{min} = a$; in y-direction: $d_{min} = a/2$; ratio = 2:1;
a = long axis; b = short axis; α = orientation of long axis, CCW from positive x-axis.

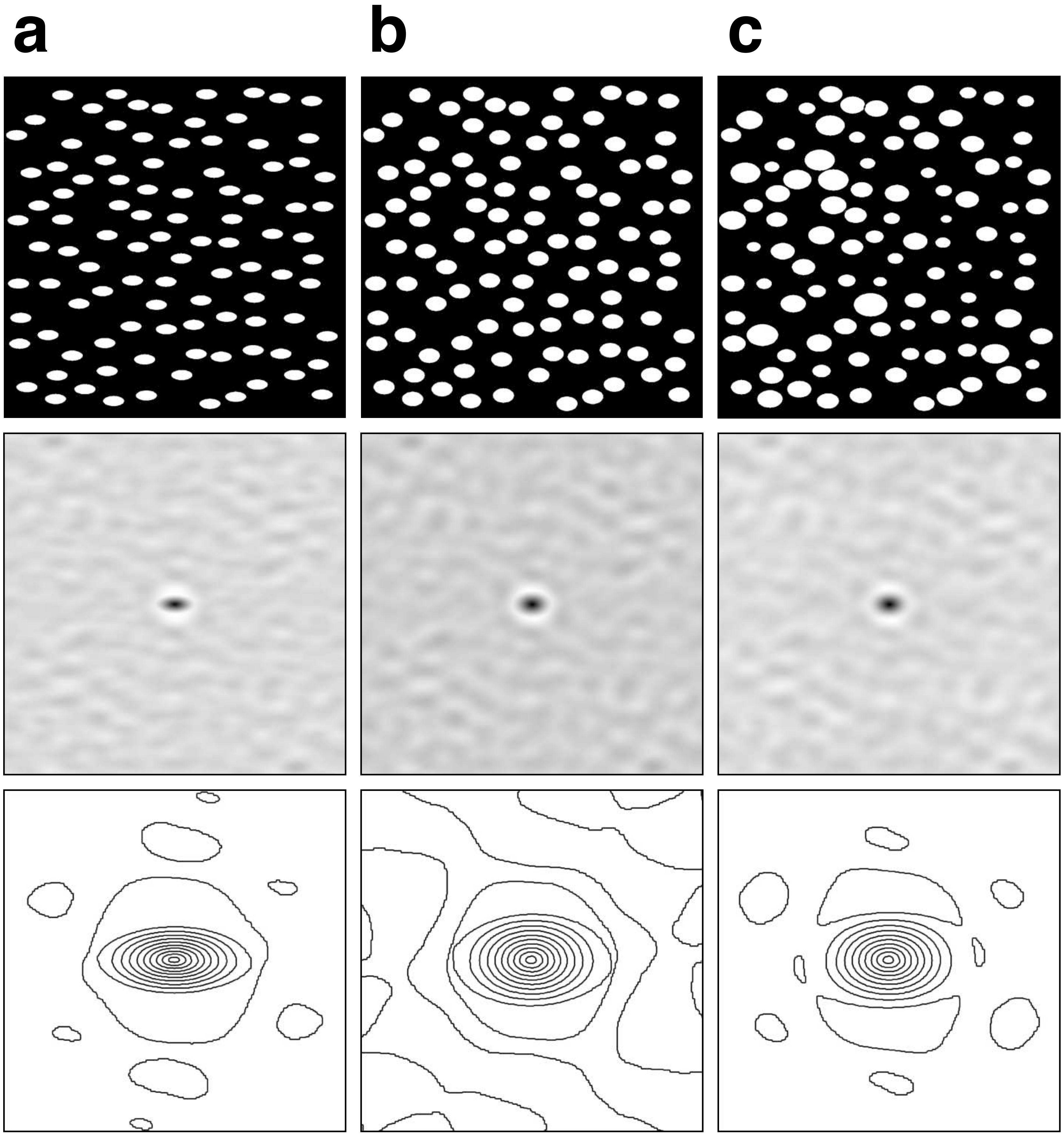

Figure 20.7
Influence of shape and size on autocorrelation function.
100 ellipses are randomly distributed in the image plane with isotropic anti-correlated distribution of center points (top). The ACF is shown at the same scale (middle) and 4 times enlarged (bottom).
(a) Constant size, b/a = 0.50, α = 0°;
(b) constant size, b/a = 0.70, α = 0°;
(c) size normally distributed; b/a = 0.70, α = 0°;
a = long axis; b = short axis; α = orientation of long axis, CCW from positive x-axis.

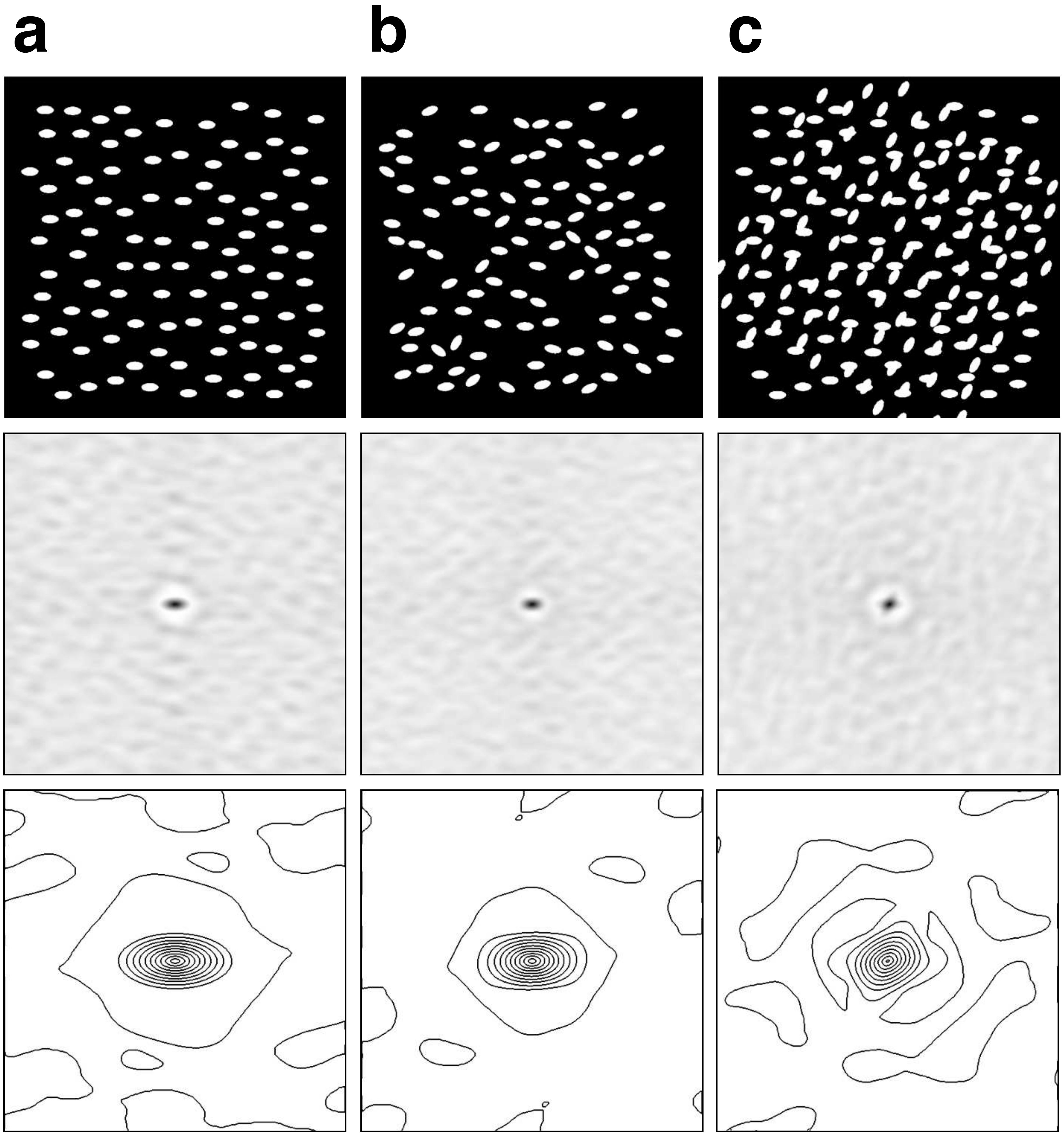

Figure 20.8
Influence of orientation on autocorrelation function.
100 identical ellipses are randomly distributed in the image plane with isotropic anti-correlated distribution of center points (top), for all, b/a = 0.50. The ACF is shown at the same scale (middle) and 4 times enlarged (bottom).
(a) Constant orientation, the orientation distribution function (ODF) is the delta function, $\alpha = 0°$;
(b) ODF = Gaussian normal distribution with, $\alpha = 0° \pm 30°$;
(c) bimodal ODF: $\alpha_1 = 0°$, $\alpha_2 = 60°$;
a = long axis; b = short axis; α = orientation of long axis, CCW from positive x-axis.

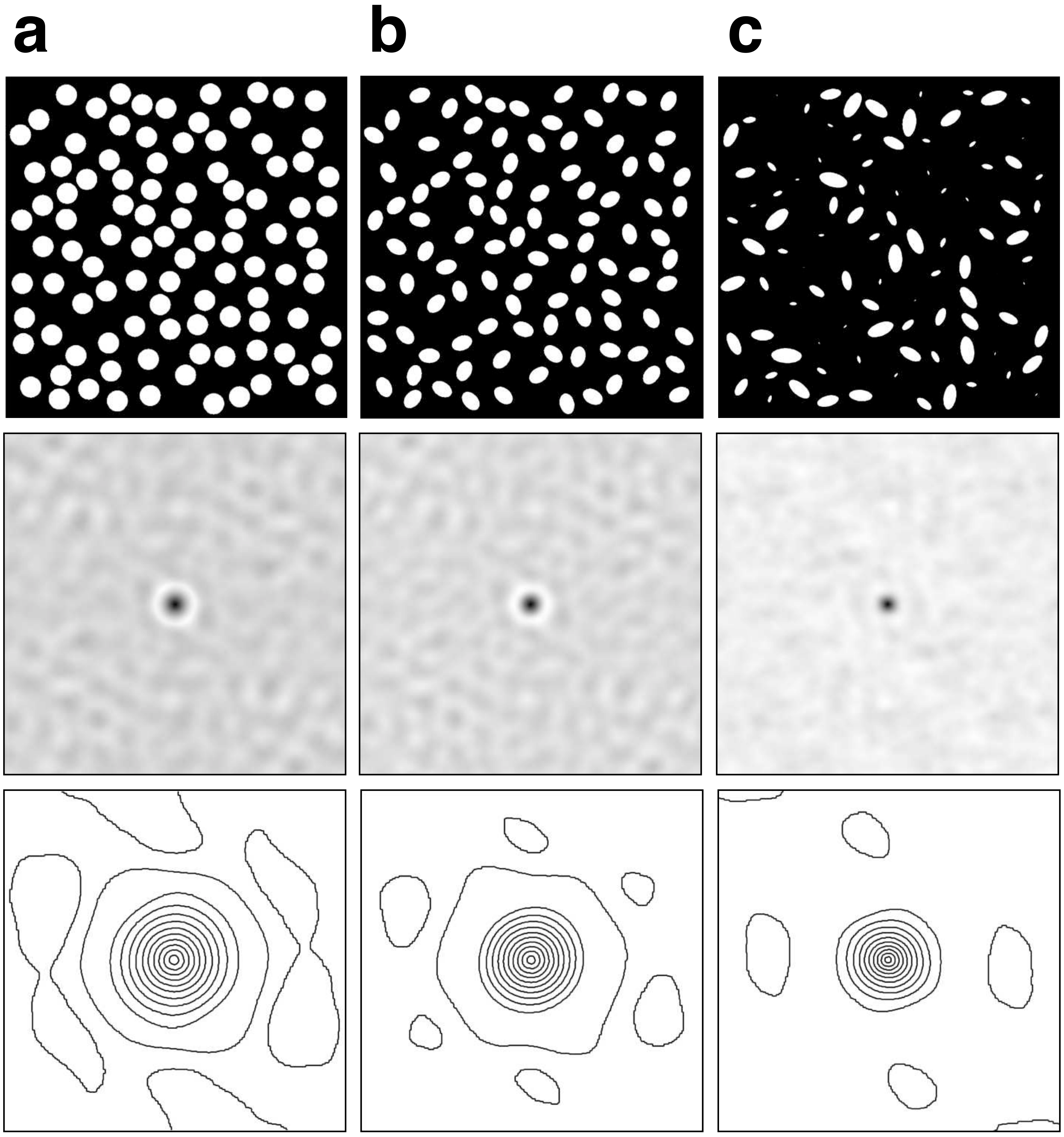

Figure 20.9
Isotropic autocorrelation functions from anisotropic shapes.
100 shapes are randomly distributed in the image plane with isotropic anti-correlated distribution of center points (top), orientation of long axes is random. The ACF is shown at the same scale (middle) and 4 times enlarged (bottom).
(a) 100 identical circles;
(b) 100 identical ellipses (b/a = 0.70);
(c) 100 ellipses with constant axial ratio (b/a = 0.50) and normally distributed size;
a = long axis; b = short axis.

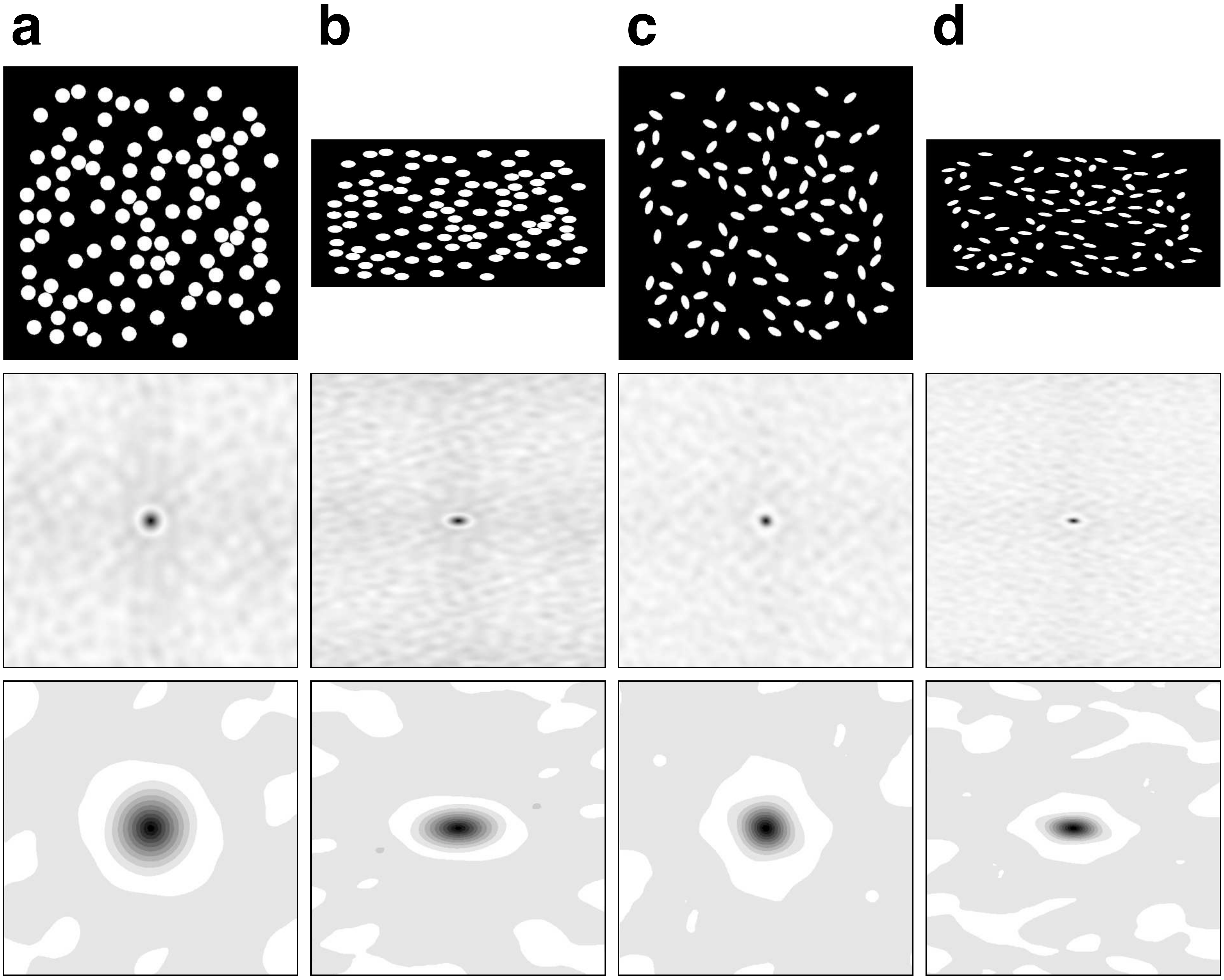

Figure 20.10
Autocorrelation and strain.
Original and strained circles and ellipses are shown (top). The ACF is shown at the same scale (middle) and 4 times enlarged (bottom).
(a) 100 circles;
(b) strained version of (a), vertical shortening to 50%;
(c) randomly oriented ellipses (b/a = 0.50);
(d) strained version of (c), same strain as in (b).

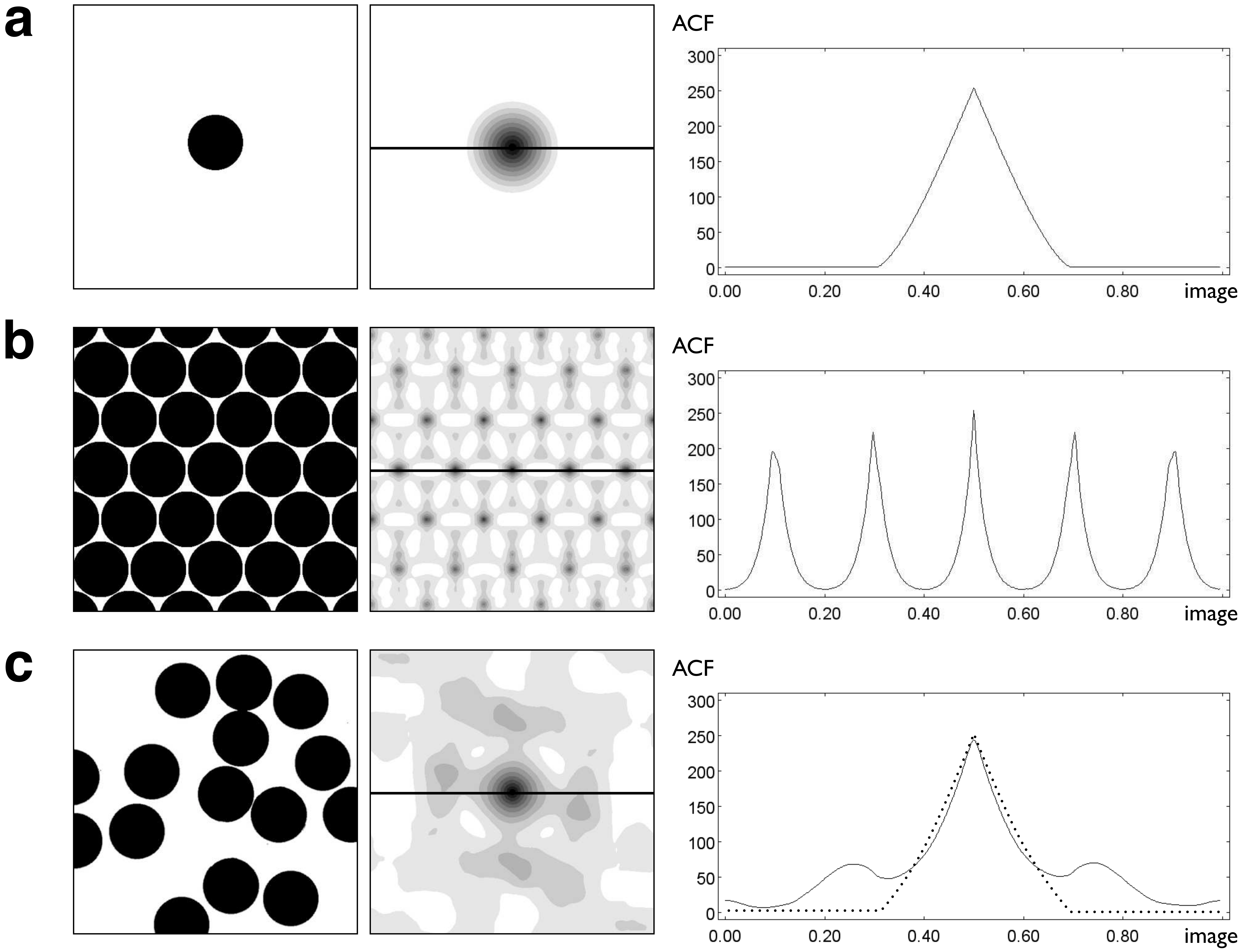

Figure 20.11
Autocorrelation function and packing density.
From left to right, the image, the ACF (both shown at the same scale), and a profile across the ACF along the indicated trace, for:
(a) a single circle;
(b) hexagonal closest packing of circles;
(c) random packing of circles; stippled line = profile of (a);
all circles have same diameter; ACF image is scaled: image width = 1; in profile, autocorrelation is given in gray values (0 - 255).

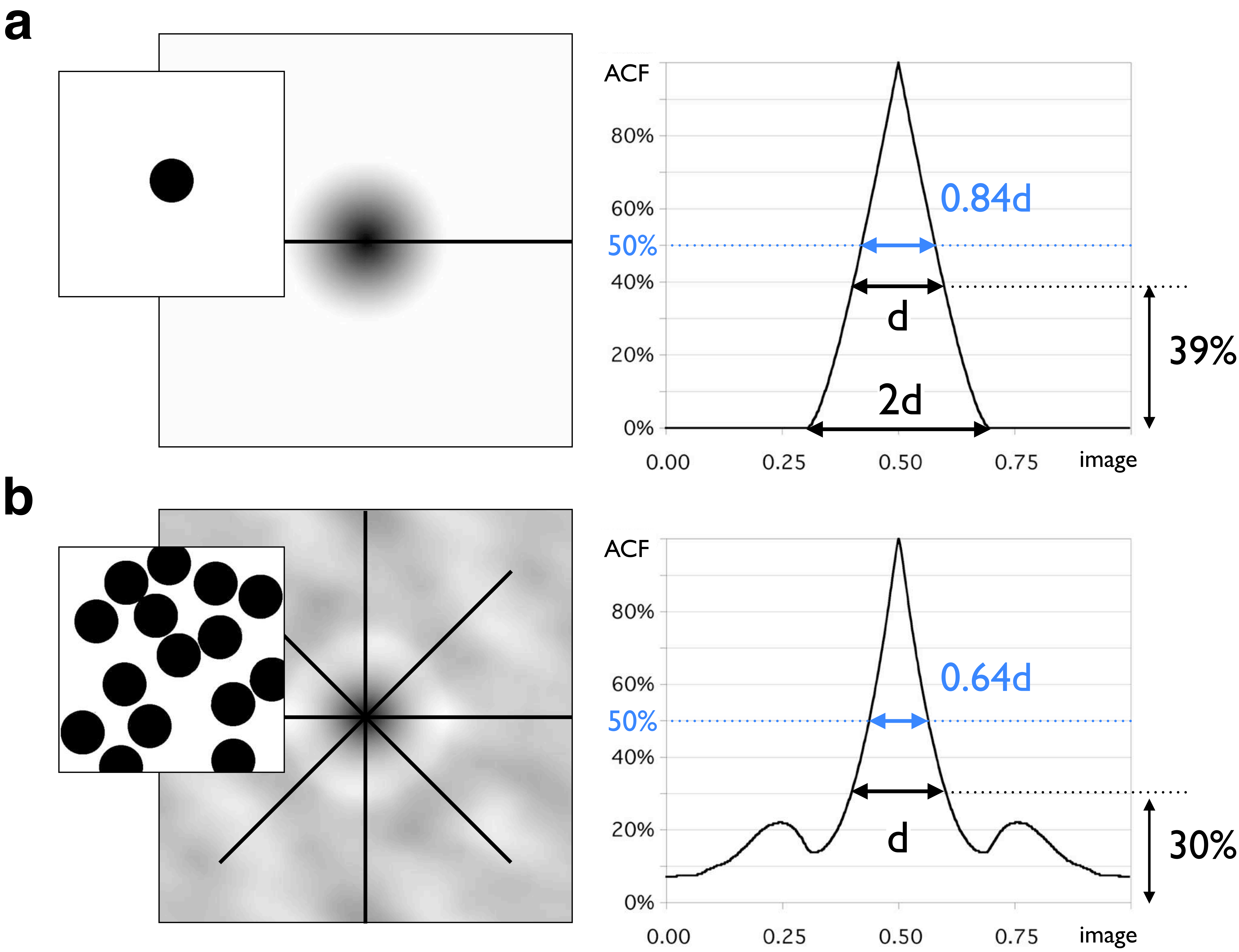

Figure 20.12
Critical levels and lengths of the autocorrelation function.
From left to right, the image, the ACF (ACF at twice the size of the image), and a profile across the ACF along the indicated traces.
(a) Single circle with diameter = d: at 50% of the ACF_{max}, the diameter of the ACF is 0.84d (blue), the level of correlation where the diameter of the ACF = d is 39%:
(b) Set of circles with diameter = d: profile = average of 4 (see traces); at 50% of the ACF_{max}, the diameter of the ACF is 0.64d (blue), the level of correlation where the diameter of the ACF = d is ~30%.

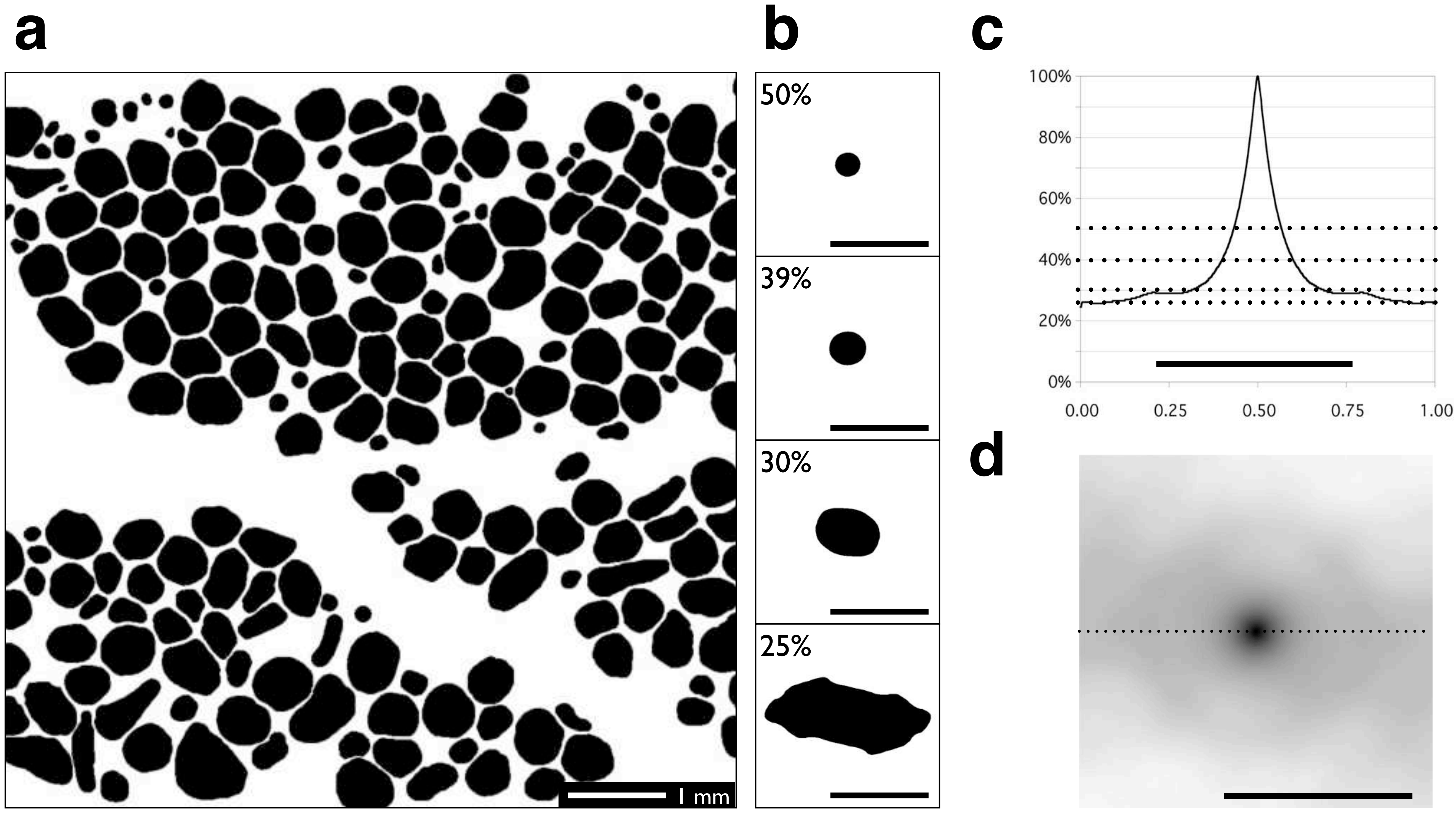

Figure 20.13
Interpreting the autocorrelation function.
The diameter of the ACF depends on the level of correlation.
(a) 1024 · 1024 bitmap of an oolithic limestone;
(b) center of ACF, thresholded at different levels
(c) profile of the ACF; selected levels (see (b)) are highlighted by heavy stipples;
(d) ACF of (a), enlarged 2x;
scale bars in (a) to (d) are same length = 1 mm.

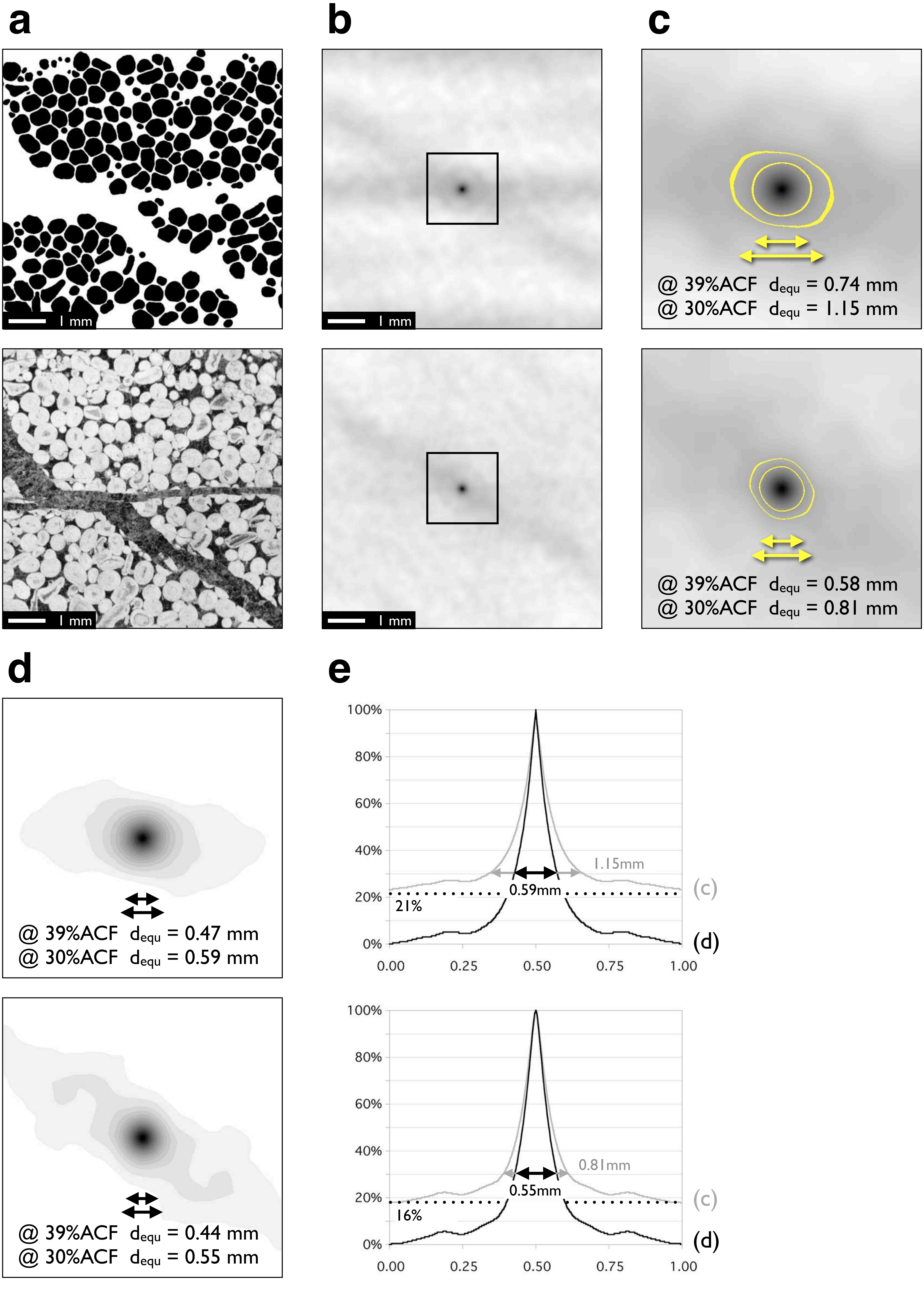

Figure 20.14
Size and level of autocorrelation.
(a) Image from which ACF is calculated: segmented bitmap (top), unsegmented original (bottom);
(b) ACF, same size as (a), box = area shown in (c);
(c) center of ACF, 4 times magnified, cross sections at 30% and 39% level in yellow, diameter indicated;
(d) center of ACF as (c) with minimum value of ACF subtracted, 20 gray values at 5% interval; diameter of cross sectional areas of ACF at 30% and 39% levels indicated;
(e) horizontal profiles though centers of (c) and (d): gray line = profile of ACF as calculated; black line = profile of ACF stretched between 0% and 100%; diameters of peak at 30% indicated.

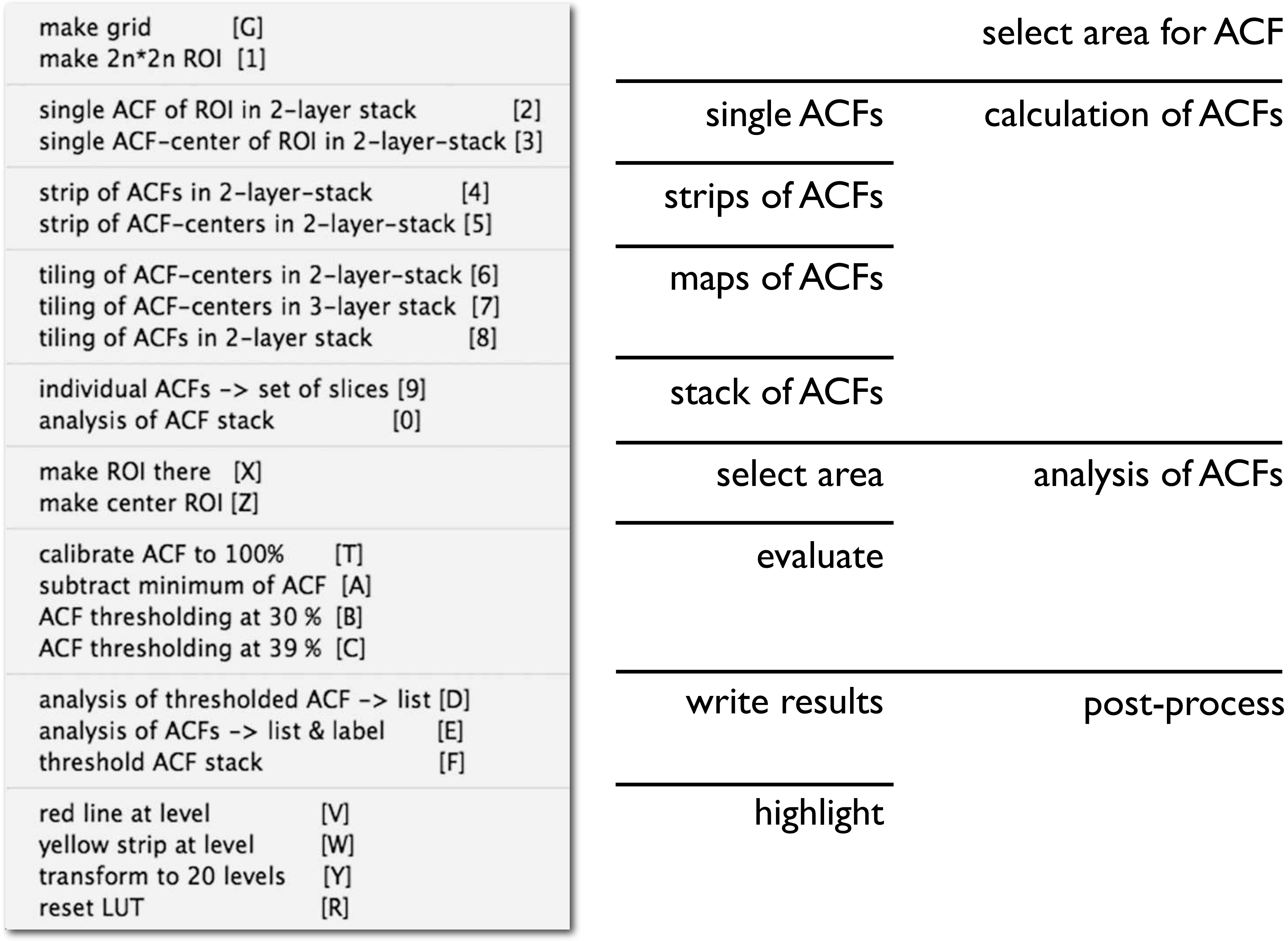

Figure 20.15
The Lazy ACF tiles macro.

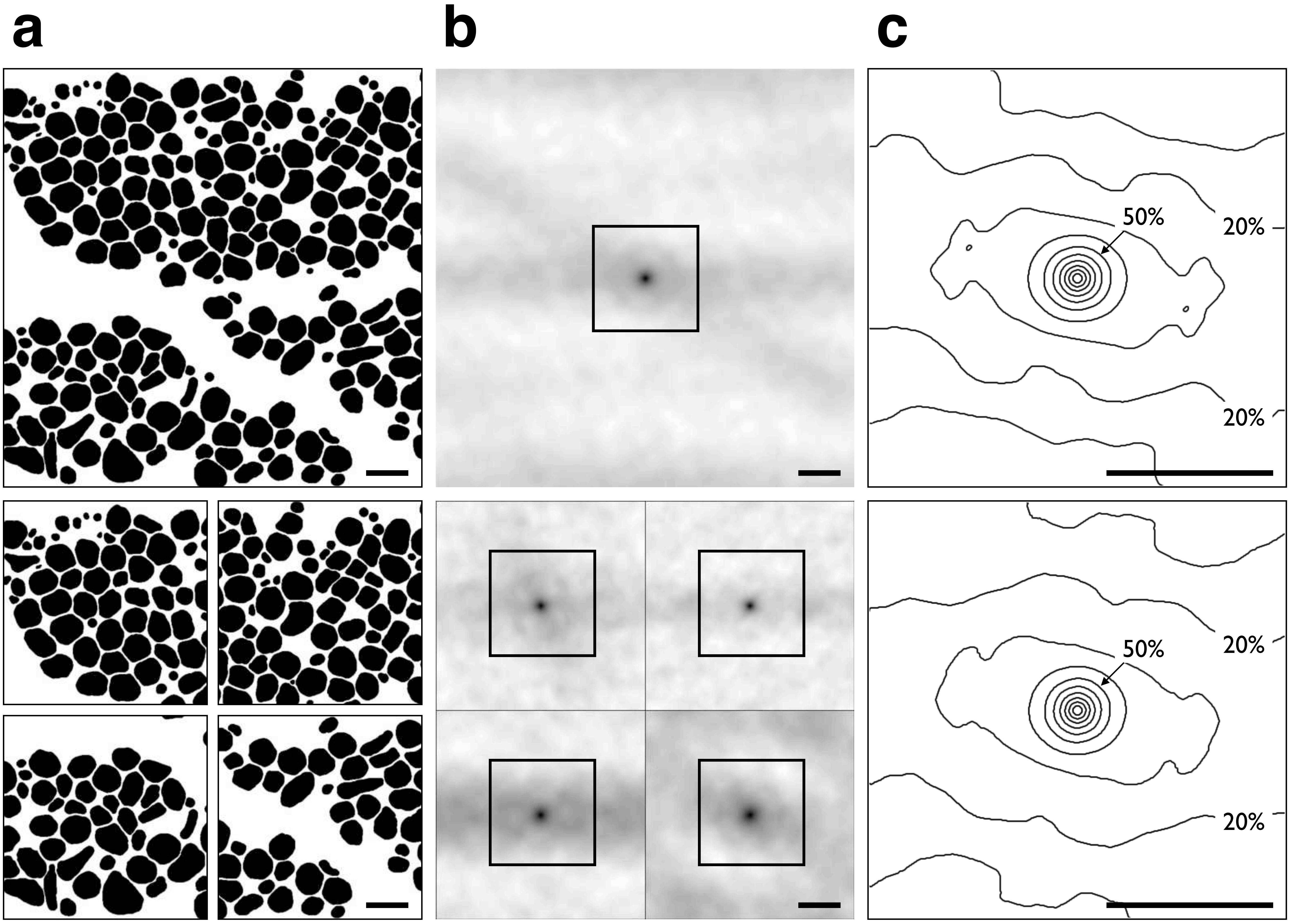

Figure 20.16
Combining autocorrelation functions of bitmaps.
The ACFs of a bitmap of an oolithic limestone is calculated in two different ways: directly (top) and by averaging the ACFs of four quarter ACFs (bottom).
(a) Single bitmap of 1024 · 1024 and 4 bitmaps of 512 · 512;
(b) 1024 · 1024 ACF and set of 4 ACFs of 512 · 512;
(c) contour plot of ACF center (256 · 256) of single ACF (top) of average of 4 ACFs (bottom).
Scale bars represent 10% of the original image width; contour levels in (c) are 10% intervals of ACF_{max}.

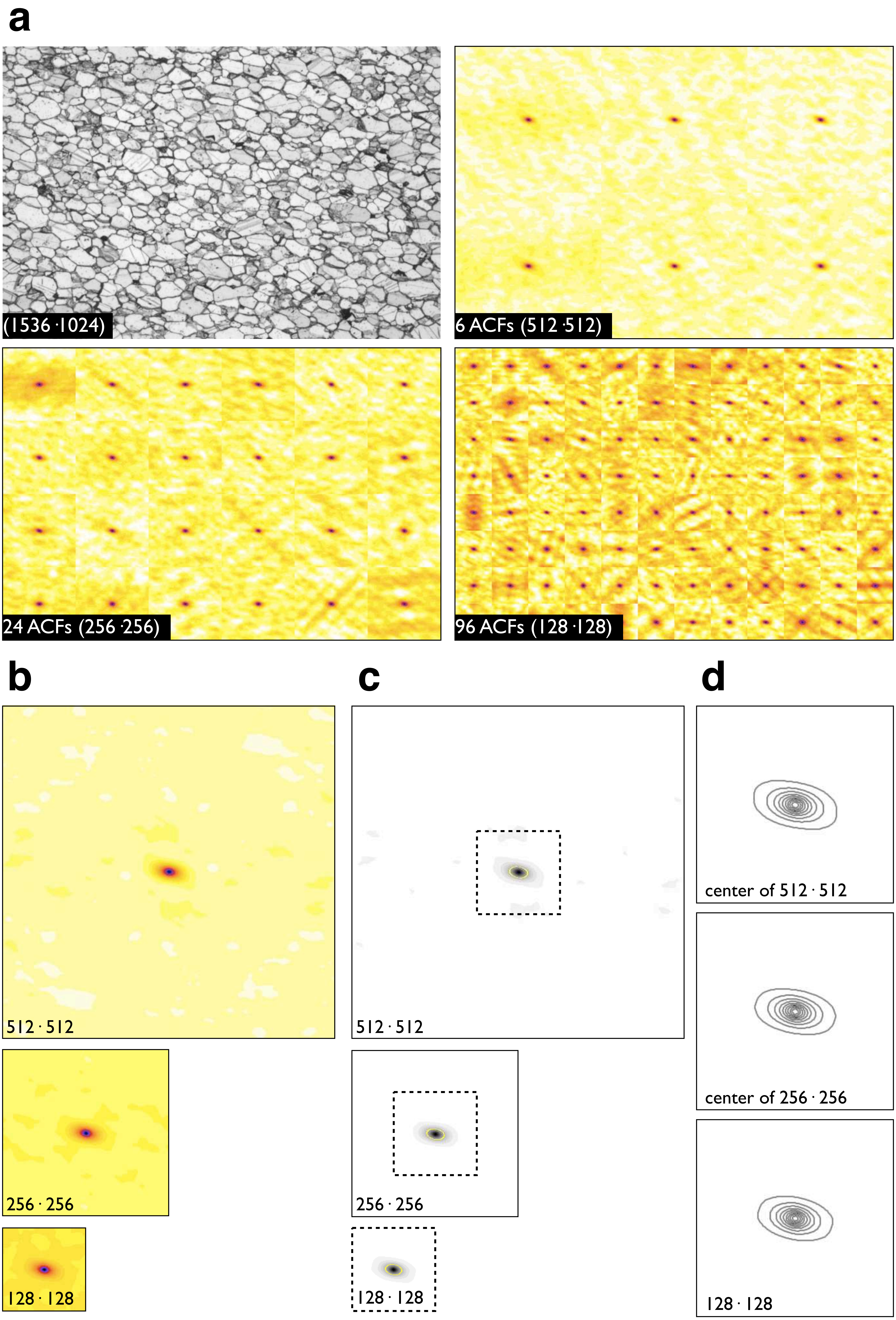

Figure 20.17
Combining autocorrelation functions of raw images.
(a) Grayscale micrograph of Carrara marble (1536 · 1024) and 3 ACF tessellations;
(b) average ACFs of tessellations shown in (a), color look-up table = 'Fire-2' LUT;
(c) average ACFs (b) with background correlation subtracted, 20 gray levels at intervals = 5% of ACF_{max}; yellow= 30% level of ACF;
(d) centers of ACFs (c), contours at intervals = 10% of ACF_{max}.

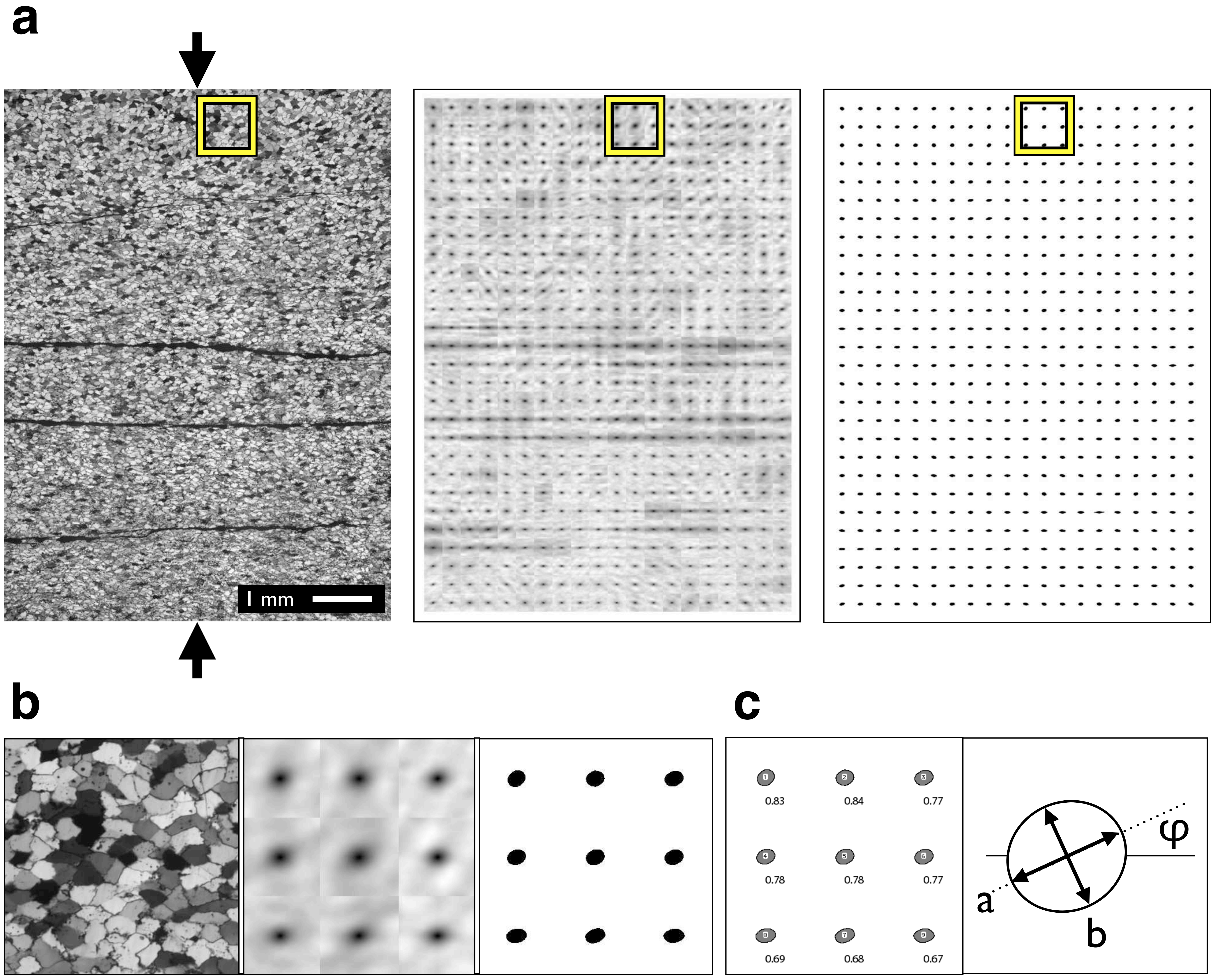

Figure 20.18
Tessellation of autocorrelation functions.
(a) From left to right, three slices of stack created with the Lazy ACF tiles macro: original micrograph of a vertically compressed Black Hills quartzite (experiment by Jan Tullis) with compression direction indicated by arrows, tessellation of ACF centers and map of thresholded ACF centers;
(b) details of (a); frame of corresponding areas are shown in (a);
(c) values of axial ratio, b/a, printed in ACF map; a = long axis, b = short axis of best-fit ellipse; φ = orientation of long axis, with respect to positive x-axis.

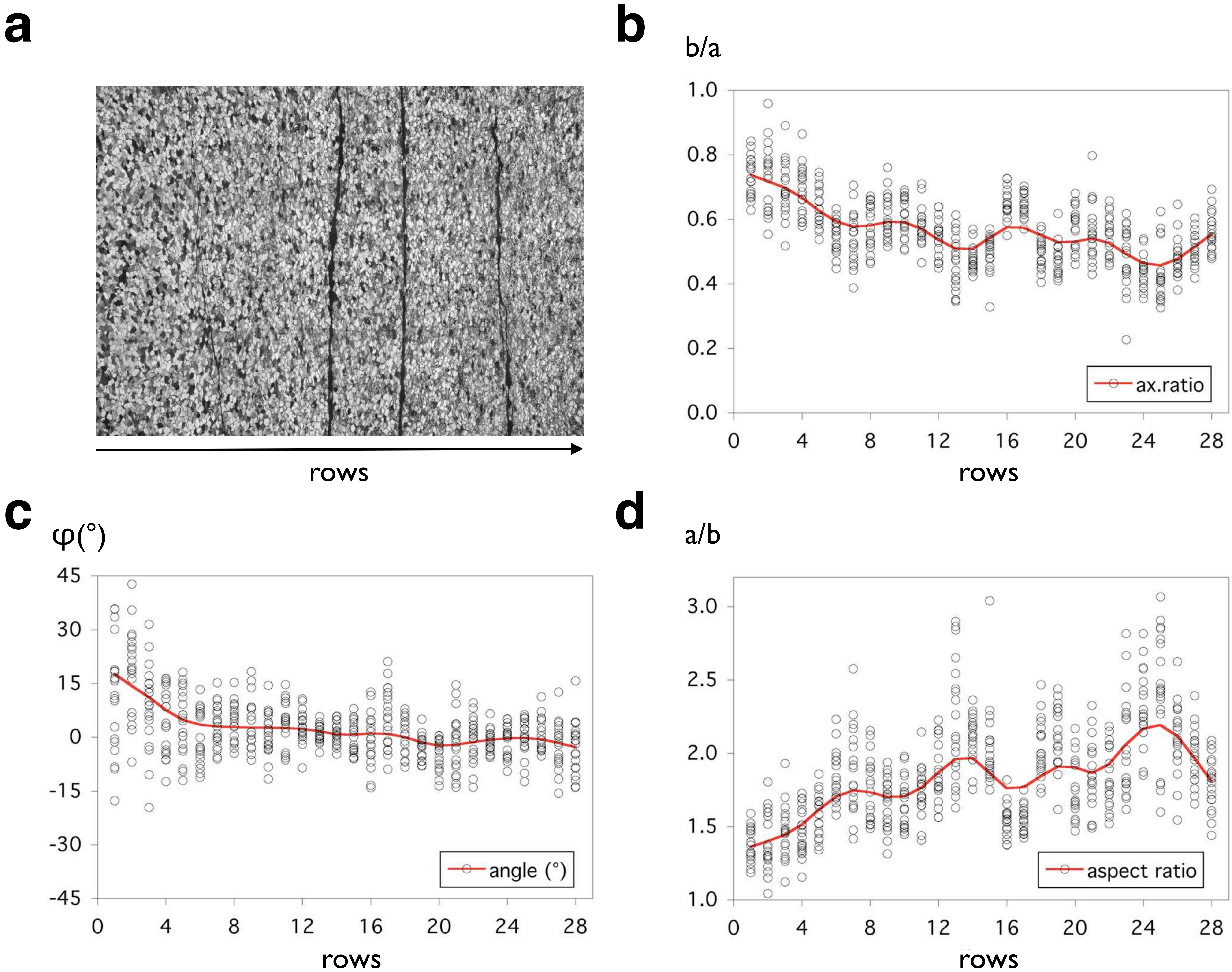

Figure 20.19
ACF mapping of experimentally deformed quartzite.
(a) Original micrograph of a vertically compressed Black Hills quartzite, rotated 90° with respect to original orientation (Figure 20.18); intensity of deformation (dynamic recrystallization) increases from left to right;
(b) plot of axial ratios, b/a;
(c) plot of angles, φ;
(d) plot of aspect ratios, R_f = a/b.

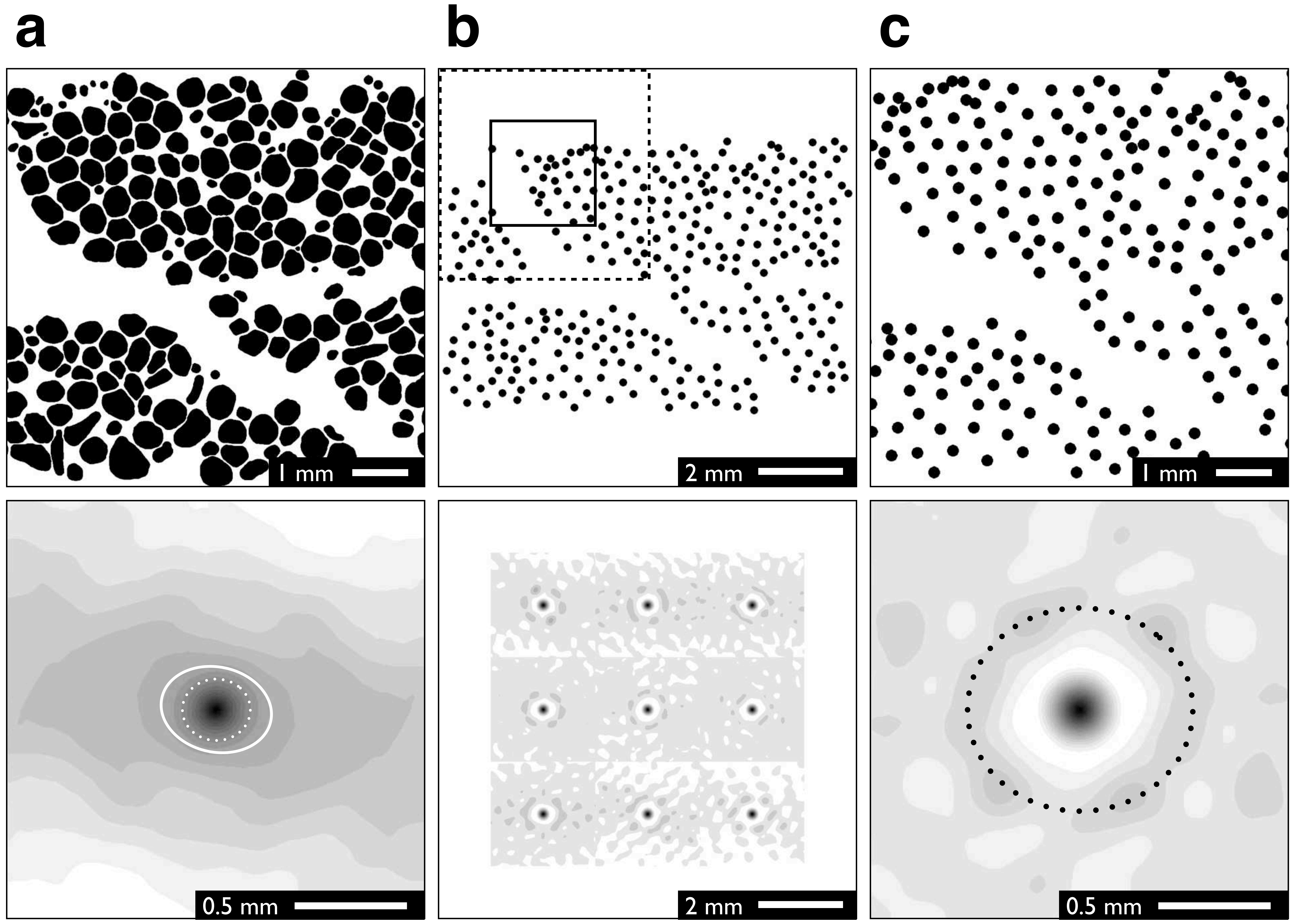

Figure 20.20
Autocorrelation of center points.
(a) 1024 · 1024 bitmap of oolithic limestone (top) and 256 · 256 center of ACF (bottom); solid outline = 30% level: b/a = 0.77, φ = 167.5°, stippled outline = 39% level: b/a = 0.914, φ = 179.9°;
(b) 1024 · 1024 bitmap of oolithic limestone covering larger area than (a) (top); map of ACF centers (bottom); solid and stippled squares indicate the center (256 · 256) and the evaluated area (512 · 512) of the first sub-region;
(c) center points of oolithic limestone shown in (a) (top) and 256 · 256 center of ACF (bottom); outlines in ACF = the anti-correlating distance;
all contour levels are 5% intervals of ACF_{max}.

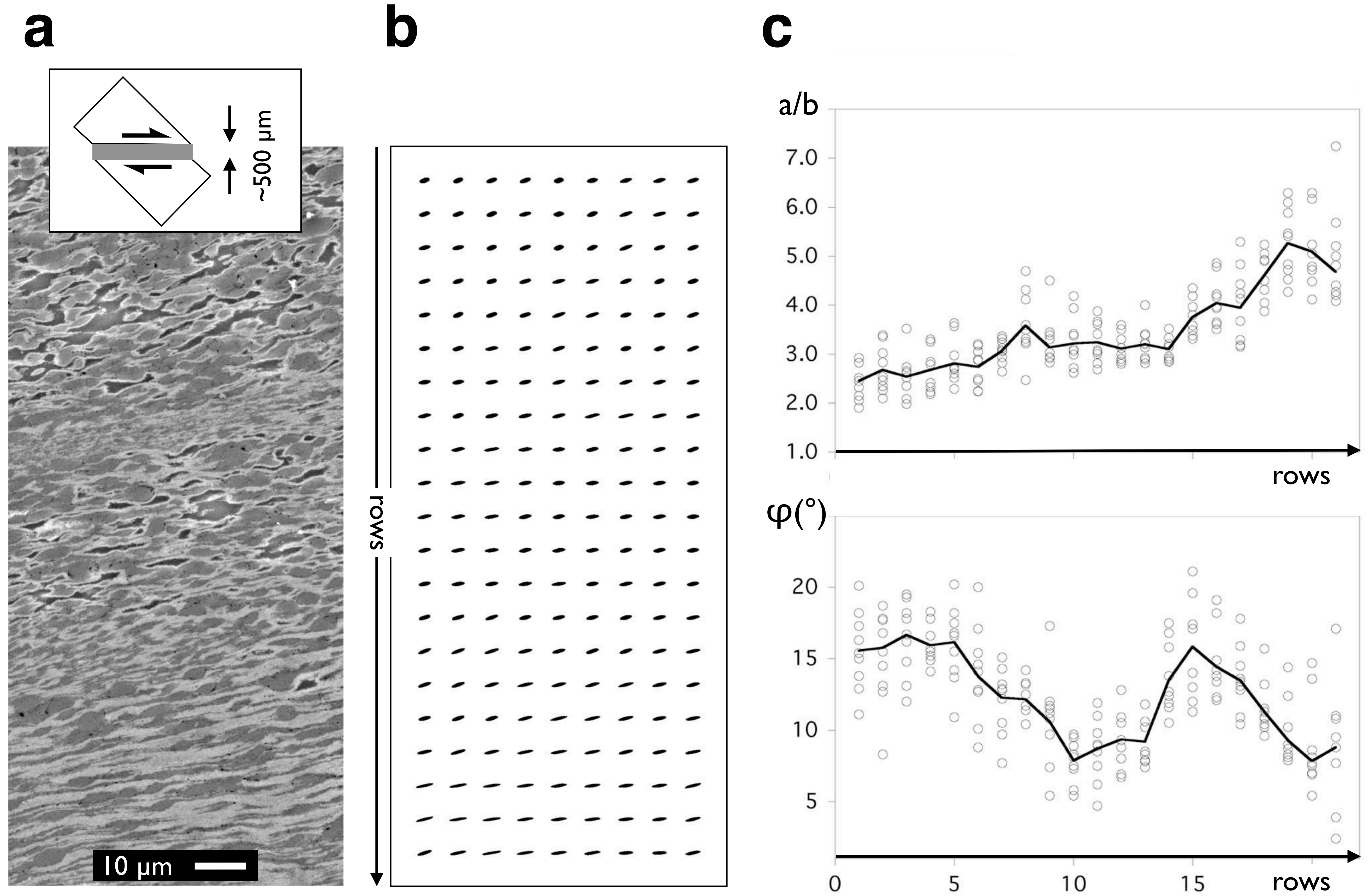

Figure 20.21
Autocorrelation of mineral phases undergoing deformation and reaction.
(a) SEM micrograph (BSE contrast) of an experimentally produced shear zone (experiment by Almar De Ronde); inset shows sample assembly, height of micrograph is ~25% of entire shear zone width;
(b) example of tessellation of thresholded ACFs (olivine, see Figure 22.a);
(c) results of evaluation (command [E] of Lazy ACF macro), plot of aspect ratios, $R_f = a/b$ (top); plot of angles, φ (bottom).

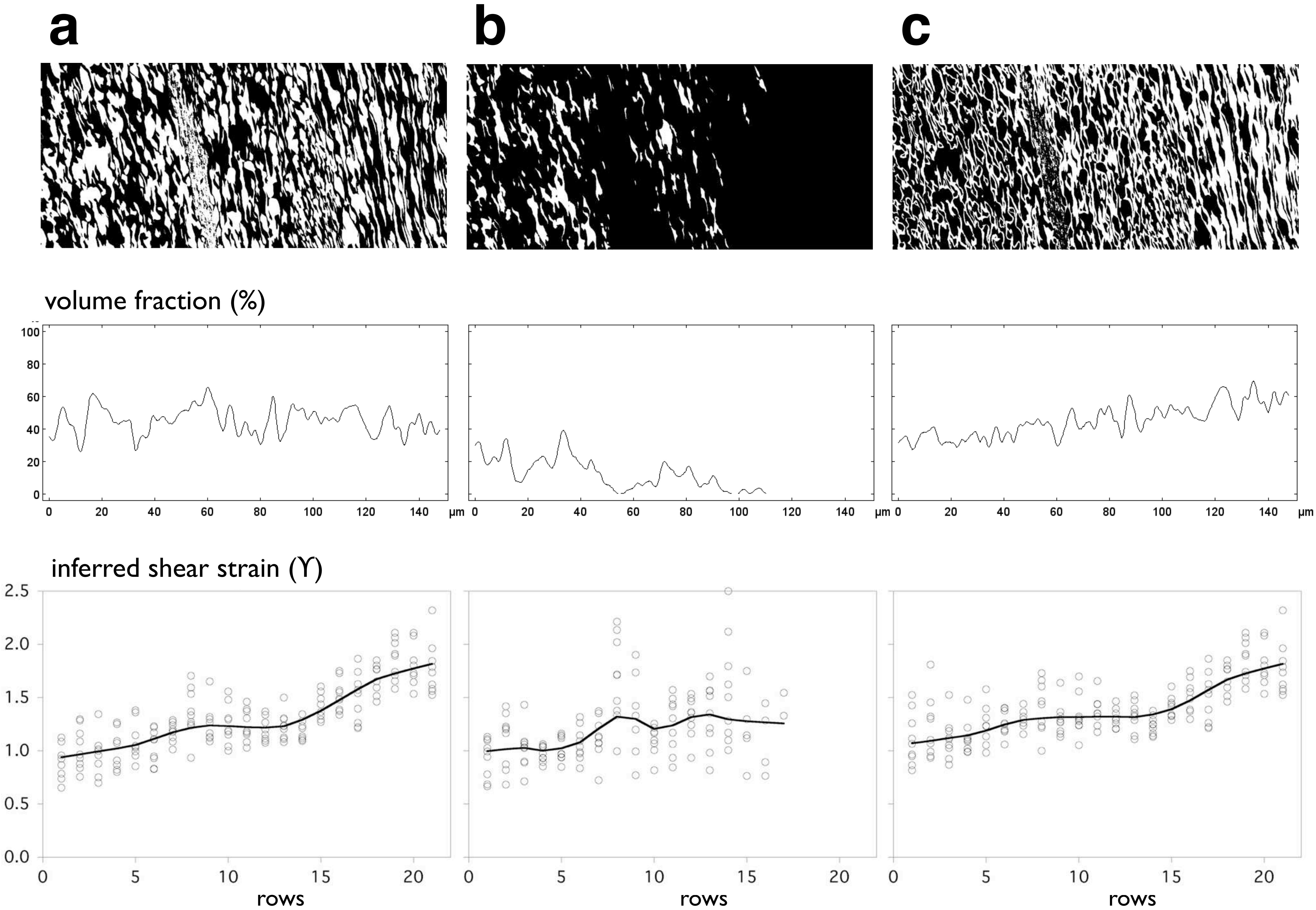

Figure 20.22

Strain interpretation of autocorrelation function.

Phase map (top), phase content (middle) and inferred shear strain, ϒ (bottom). Volume content is from profile of bitmap convolved with 15 · 15 Gauss filter kernel; shear strain is derived from aspect ratio as $\Upsilon = (R_f - 1) / \sqrt{R_f}$ where = a/b, a = long axis, b = short axis of best-fit ellipse (see Figure 20.21).

(a) Olivine;

(b) plagioclase;

(c) reaction products.